Electrochemical-Impedance-Spectroscopy Study of Corrosion of the Alloy NF616 with Molten ZnCl₂-KCl Coating in Air at 673 K

T. J. Pan, 1,2,* W. L. Xue, D. G. Chen and J. Hu

- ¹ School of Materials Science and Engineering, and Key Laboratory of Advanced Metallic Materials of Changzhou City, Changzhou University, China
- Wei Hua Precision Alloy Co., Ltd. Jiangsu, Lu Town Industrial Park, Danyang City, China

Abstract. The corrosion behavior of the alloy NF616 covered with a film of molten 0.55ZnCl2-0.45KCl (mole fraction), similar to that found in waste incineration plants, was examined in air at 673 K by the electrochemicalimpedance spectroscopy (EIS) technique. For comparison, the corrosion of the same material immersed in the deep salt was also studied. The electrochemical impedance spectra for the corrosion of NF616 beneath a film of fused salt consisted of a semi-circle at high-frequency port and a line at low-frequency port indicating a diffusion-controlled reaction. Contrary to the corrosion beneath salt film, the corrosion of the alloy in deep molten salt presented the characteristics of two capacitive loops during all the duration of the experimental test. This different EIS features under two corrosion conditions may be related to the different supply of oxygen amount. In this paper, suitable equivalent circuits representing the corrosion of the alloy under the two different corrosion conditions are proposed to fit the corresponding impedance spectra and electrochemical parameters in the equivalent circuits are also calculated.

Keywords. NF616, ZnCl₂-KCl, impedance models, electrochemical impedance.

PACS®(2010). 6000.

1 Introduction

The corrosion problems encountered in waste incineration plants often resulted from gas phase attack by HCl and chlorine gas formed beneath deposits, as well as molten salt

Corresponding author: T. J. Pan, School of Materials Science and Engineering, Changzhou University, Changzhou City, 213164, China; E-mail: tjpan2005@gmail.com.

Received: August 2, 2010. Accepted: August 27, 2010.

attack by metal chlorides and their eutectic mixtures that melt at surface of metallic materials in the operation temperature range of superheater tubes [1]. High contents of heavy and alkali metal chlorides (such as SnCl2, PdCl2, ZnCl2, KCl and NaCl), which exit usually in form of lowmelting eutectic, are particularly destructive to destroy the protective oxide scales formed on high temperature materials, even at temperatures well below the melting points of the salts. This corrosion induced by eutectic chlorides has been identified as the main degradation in waste incineration plants. This type of corrosion is actually an accelerated oxidation of materials covered with a thin film of fused salt exposed to an oxidizing gas atmosphere at elevated temperatures. It differs largely from the corrosion of the materials in deep salt. However, this hot corrosion occurs mainly by an electrochemical mechanism, because the fused salts are usually excellent ionically conducting electrolytes exhibiting acid/base chemistry. Therefore, it may be investigated by electrochemical techniques.

Generally, use of electrochemical methods such as freecorrosion potential, scanning polarization, cyclic voltammetry and linear-polarization resistance may not be sufficient to elucidate the complicated reaction processes occurring in hot corrosion. However, compared with these measurement techniques, EIS has smaller disturbance to the system, and moreover has proved effective in understanding the reaction mechanisms and kinetics, and obtaining more information concerning the corrosion processes. Thus, electrochemical impedance studies of hot corrosion under a thin salt film are necessary for the eventual understanding of corrosion kinetics and corrosion mechanisms. Since the 1980s, EIS has been applied to the study of hot corrosion [2–10]. In general, a successful application of the EIS technique in hot corrosion requires suitable models for fitting the impedance spectra. Zeng et al. [5] ever used EIS technique to investigate the molten-salt corrosion behavior by proposing four models to describe the scaling features of metallic materials. Moreover, Test-cell design is also important to electrochemical measurements of corrosion of materials covered with a thin film of molten salts. A two-electrode arrangement comprising two working electrodes can be prepared conveniently, and is also suitable for simple electrochemical impedance measurements [9,10]. In a previous study [11], the present author employed a twoelectrode system to study the corrosion behavior of Ni and Fe in the presence of a salt film at 673 K in air, respectively. The different EIS features were observed for the hot corrosion of Ni and Fe. This difference between in deep salt and beneath molten salt film may be related to the scale formed on the alloy surface and the consumption of the fused salt.

However, up to now, the studies on hot corrosion by using EIS technique are still limited. In the present work, the corrosion behavior of NF616 covered with a thin film of molten ZnCl₂-KCl at 673 K in air was investigated by using EIS technique, with the emphasis on the impedance measurement and the establishment of impedance models for a thin salt film induced hot corrosion.

2 Experimental Procedures

The material used in this study is the Fe-based alloy NF616 with the following chemical compositions: Fe-9.0Cr-0.1C-0.11Si-0.5Mn-0.4Mo-1.8W-0.2V (in mass %). Electrochemical impedance measurements were carried out in molten salt at 673 K in air by using the experimental apparatus reported early [11] and the experiment process is also described early in reference [11]. The working electrodes were prepared as follows. Samples of the alloy were machined into a size of $10 \times 10 \times 5$ mm³, and then each sample was ground down to 600#SiC paper. A Ni-Cr wire was spot welded to one end of the specimens for electric connection. Two specimens very closely spaced were sealed in an alumina tube by high temperature cement. The exposed surfaces of the specimens were in the same plane. After the cement was dried at room temperature, it was further solidified at 473 K for 24 h. The working electrode surface was polished again on 600#SiC paper, degreased and dried.

A mixture of 0.55ZnCl₂-0.45KCl (molar ratio) was applied in the present study. A total of 160 g of the salt mixture were dried in an alumina crucible at 473 K for 24 h in air. Then, the furnace was heated to 673 K. In order to produce a thin fused salt film on the electrode surface, the electrode arrangement was immersed briefly into the melt, then withdrawn and kept above the melt. The actual amount of the thin salt film was about 2 mg/cm² in this present study.

Electrochemical impedance measurements were performed at open-circuit potential in air between 0.01 and $1x10^5$ Hz with a M398 impedance system, composed of a Princeton Applied Research (PAR) 5210 lock-in amplifier and a PAR 263 potentiostat interfaced through an IEEE 488 bus to a compatible computer. A fast Fourier transform (FFT) technique was employed for frequencies from 0.01 to 1.13 Hz to increase measurement speed and lower the degree of perturbation to the cell. The amplitude of input sine signal was 10 mV. A commercial software (ZSimpWin) developed by Princeton Applied Research was used to fit the impedance spectra. In the end, the corroded specimens were analyzed by X-ray diffraction and scanning electron microscopy coupled with EDAX.

3 Experimental Results and Discussions

3.1 Results of EIS Measurements

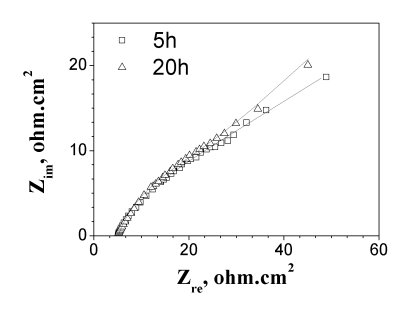
The typical Nyqusit and Bode plots for corrosion of the alloy NF616 beneath a thin fused salt film and in deep molten salt after different exposure time are shown in Figure 1 and Figure 2, respectively. The impedance spectra for corrosion of NF616 beneath a salt film are very similar during the whole experimental duration. The Nyquist plots are composed of a depressed semi-circle at high frequency and a line at low frequency, indicating a diffusion-controlled reaction. Moreover, the corresponding Bode plots show only a time constant. However, the impedance features for corrosion of NF616 in deep molten salt differed from that beneath salt film. The Nyquist plots were composed of a small capacitive loop at high frequency and a relative large capacitive loop at low frequency. Furthermore, the corresponding Bode plots obviously show two time constants.

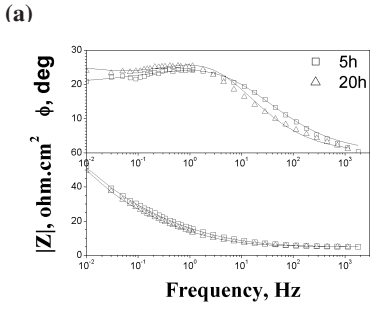
3.2 Scale Morphology

Back-scattered electron images of the cross-sectioned NF616 alloy corroded below a fused salt film and in deep salt are shown in Figure 3. The corrosion product formed beneath a salt film comprised an outer layer of iron oxide (Fe₂O₃) with presence of some zinc (2-3 at. %), potassium (1-2 at. %) and chlorine (2-3 at. %), and an inner layer of mixed iron-chromium oxide again containing similar contents of Zn, K and Cl. Moreover, the scales were rather porous and also exhibited distinctive separations. A small amount of chlorine was detected by EDS analysis at the scale/alloy interface. The corrosion product formed in the deep salt is shown in Figure 3(b) The microstructure was substantially similar to that formed beneath salt film (Figure 3(a)), but much thinner. The scale also composed of a porous outer layer of iron oxide and a relative compact Cr-rich inner layer. The scale also contained some zinc (1-3 at. %), potassium (2–3 at. %) and chlorine (3–4 at. %). Only a small amount of chloride (CrCl₂ and FeCl₂) can be detected at scale/alloy interface by EDS analysis because a large amount of chloride from the dissolution of NF616 in chlorides substantially changed into the corresponding oxide (Fe₂O₃ and Cr₂O₃) in air when the corroded samples was drew out from deep salt, which is mainly because the oxide is the stability phase in air according to the phase diagrams [12].

3.3 Impedance Models and Discussion

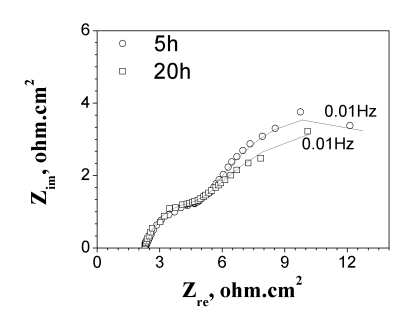
Due to the two electrode arrangement, the impedance responses may come from the contributions of the corrosion system. The impedance results represent the responses from the corroding specimens, including the contributions from the electrochemical charge transfer process, diffusion, and the scale formed on the alloy surface.

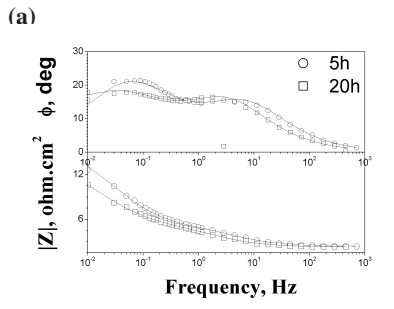




(b)

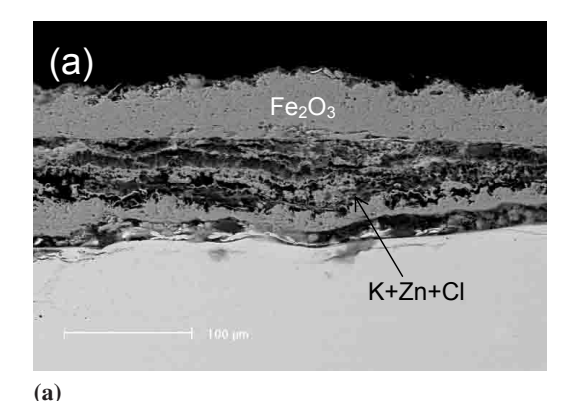
Figure 1. Nyquist and Bode plots for the corrosion of NF616 covered with a film of ZnCl₂-KCl melt in air at 673 K after different exposure times, symbol: experimental data; line: simulation data.





(b)

Figure 2. Nyquist and Bode plots for the corrosion of NF616 immersed in the deep melt of ZnCl₂-KCl mixture in air at 673 K after different exposure times, symbol: experimental data; line: simulation data.



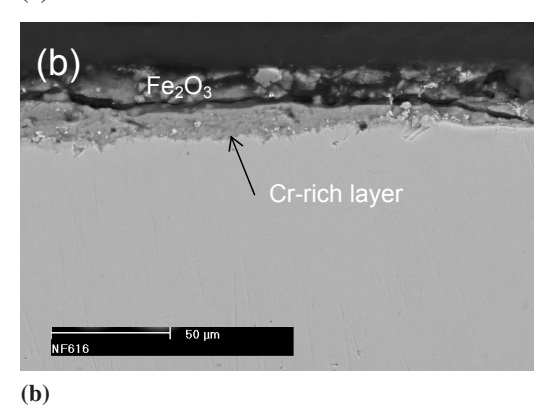


Figure 3. Micrographs for cross sections of NF616 at 673 K in air for 24h beneath salt film (a) and in deep salt (b).

The Nyquist plots for corrosion of NF616 beneath fused ZnCl₂-KCl film obviously show the feature of diffusion-controlled reaction. Thus, an equivalent circuit of Figure 4(a) was proposed to fit the impedance plots. However, the Niquist plots for the corrosion of NF616 in deep molten ZnCl₂-KCl presented two capacitances, i.e., a much larger semicircle at low frequency and a small depressed semicircle at high frequency. The impedance spectra may be associated with the growth of porous scales on the surface of the NF616 alloy. At this state, the molten salt can penetrate inward along the micropores in the scale to the metal matrix to induce electrochemical reaction. Thus, the corrosion of the alloy in deep molten salt can be described by the equivalent circuit of Figure 4b.

In Figure 4, R_s represents the electrolyte resistance, $C_{\rm dl}$ the double-layer capacitance, $R_{\rm t}$ the charge-transfer resistance, $Z_{\rm w}$ the Warburg resistance. In Figure 4b, $C_{\rm p}$ and $R_{\rm p}$ represent the porous scale capacitance and the pore resistance, respectively. $C_{\rm dl}$ and $R_{\rm t}$ again represent the double-layer capacitance and the charge-transfer resistance at the electrolyte/metal interface formed by the inward penetration of molten salts along pores, respectively. Taking into account the dispersion effect, a constant phase angle element (CPE) Q was used to describe the element $C_{\rm dl}$ and $C_{\rm p}$ in the fitting procedure. Thus, the total impedance of

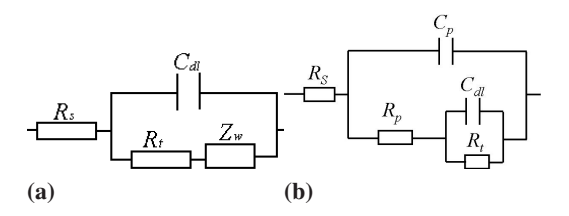


Figure 4. Equivalent circuit representing the corrosion of NF616 in ZnCl₂-KCl mixture at 673 K in air.

Figure 4a can be expressed by the following equation (1):

$$Z = R_s + \frac{1}{Y_{dl}(j\omega)^{n_{dl}} + \frac{1}{(R_i + Z_w)}}$$
(1)

Where $Z_{\rm w}$ represents the Warburg resistance related with the diffusion of the oxidant species. The Warburg resistance $Z_{\rm w}$ may be expressed by the following equation (2):

$$Z_w = A_w (j w)^{n_w}. (2)$$

Where $A_{\rm w}$ is the modulus of $Z_{\rm w}$, and $n_{\rm w}$ the Warburg coefficient, ranging between -0.5 and 0, depending on the diffusion direction of the oxidant. When $n_{\rm w}$ is equal to -0.5, the diffusion direction of the oxidant is parallel to its concentration gradient. When $n_{\rm w}>-0.5$, the diffusion direction of the oxidant deviates from its concentration gradient, i.e., "tangential diffusion". Correspondingly, the slope of the low-frequency line in Nyquist plot is less than 1. In moltensalt corrosion, the "tangential diffusion" may be related to the porosity of the scale.

In addition, the total impedance of Figure 4b can be expressed by the following equation (3):

$$Z = R_{\rm s} + \frac{1}{Y_{\rm p}(j\omega)^{n_{\rm p}} + \frac{1}{R_{\rm p} + \frac{1}{Y_{\rm dl}(jw)^{n_{\rm dl}} + \frac{1}{R_{\rm r}}}}}$$
(3)

where $Y_{\rm dl}$ and $n_{\rm dl}$, and $Y_{\rm p}$ and $n_{\rm p}$ are also constants representing the parameters $Q_{\rm dl}$ and $Q_{\rm p}$, respectively.

The parameters in equations (1)–(3) were obtained by fitting the impedance spectra on the basis of the equivalent circuits of Figure 4, and are listed in tables 1 and 2, respectively. Figs.1 and 2 show that the fitting results are quite good, indicating the proposed equivalent circuits are reasonable.

Table 1 show that the parameters $R_{\rm s}$ underwent slight changes with exposure time, possibly related to changes of the salt film on the samples. In the case of salt film corrosion, $A_{\rm w}$ is a little larger than $R_{\rm t}$, indicating that the diffusion impedance cannot be neglected. But in Table 2, the small value of $R_{\rm t}$ indicated the electrochemical reaction is very fast in deep salt. The value of $R_{\rm p}$ represents a protection of the scale. The slight change of the scale resistance

 $R_{\rm p}$ with time may be related to the dissolution of the scale formed on the alloy surface in the chloride, and the change of the scale/melt interface. In addition, the value of $n_{\rm dl}$ and $n_{\rm p}$ deviate greatly from 1, showing the presence of a dispersion effect, $n_{\rm w}$ also deviates greatly from -0.5, indicating the existence of significant tangential diffusion. This is mainly because the presence of a porous oxide scale on the surface of alloy may produce the non-uniform electric field, and thus give rise to the obvious dispersion effect. Moreover, this kind of corrosion product may also affect the diffusion direction of oxidants, and therefore lead to tangential diffusion. In fact, the dispersion effect and tangential diffusion are very significant in molten-salt corrosion.

The distinct impedance responses under the two corrosion conditions may be related to the different supply of oxidants to the alloy surface because molecular oxygen diffusion to the alloy surface is relatively difficult in deep salt, as compared to the fused salt film condition. In the presence of a film of fused KCl-ZnCl₂, oxygen can reach easily the alloy surface to contribute to the rapid conversion of formed FeCl₂ into Fe₂O₃ according to the following reactions:

$$2FeCl_2 + \frac{3}{2}O_2 = Fe_2O_3 + 2Cl_2 \tag{4}$$

In fact, the corrosion of the alloy under salt film is considerably rapid; so that the corrosion rate of the alloy is controlled by the diffusion of gaseous FeCl₂ and oxygen through the porous scales [13, 14]. Thus, the corresponding electrochemical impedance spectra show the diffusion-limited reaction.

However, for the corrosion in deep molten KCl-ZnCl₂, the alloy is only oxidized according to the following anodic reaction:

$$Fe = Fe^{2+} + 2e^{-}$$
 (5)

$$Cr = Cr^{3+} + 3e.$$
 (6)

The corresponding cathodic reaction only occur as follows:

$$\frac{1}{2}O_2 + 2e - = O^{2-}. (7)$$

The activity of oxygen in deep salt decrease because oxygen take part in the reduce reaction at the cathodic region. However, during the electrochemical reaction the rapid anodic reaction needs to consume a large amount of oxidants. Therefore, the insufficient supply of oxygen in deep salt to the cathodic reaction retards the whole electrochemical reaction because of the considerable small solubility of oxygen in chlorides, so the diffusion of the oxidant through the micropores in the scale to the alloy-melt interface may be rate limiting. Thus, the corrosion of the alloy in deep salt is limited by the supply of oxygen at the cathodic reaction.

Time	$R_{\rm s}$	$R_{\rm t}$	$Y_{o,dl}$ $(\Omega^{-1}.cm^{-2} S^{-n})$	$n_{ m dl}$	A _w	-n _w
(hr)	Ω .cm ²)	$(\Omega.cm^2)$	(22 '.cm 2 S ")		$(\Omega.cm^2S^n)$	
2	5.48	8.31	1.00e-2	0.62	21.38	0.26
5	4.96	8.33	1.11e-2	0.62	22.07	0.27
10	5.62	4.02	1.12e-2	0.63	24.31	0.25
15	5.20	4.39	1.34e-2	0.61	24.75	0.24
20	5.12	5.30	1.88e-2	0.66	23.58	0.33
24	5.03	5.11	2.41e-2	0.62	22.24	0.34

Table 1. Fitting results of the impedance spectra of NF616 covered with salt film at 673 K.

Time (hr)	$R_{\rm s}$ ${\mathfrak o}\Omega.{\rm cm}^2)$	$R_{\rm t}$ $(\Omega.{\rm cm}^2)$	$Y_{o,dl}$ $(\Omega^{-1} \cdot \text{cm}^{-2} \text{ S}^{-n})$	$n_{ m dl}$	$R_{\rm p}$ $(\Omega.{\rm cm}^2)$	$(\Omega^{-1} \cdot \text{cm}^{-2} \text{S}^{-n})$	n _p
2	2.36	2.38	3.83e-2	0.73	11.93	3.12e-1	0.68
5	2.27	1.85	7.039e-2	0.77	14.25	3.95e-1	0.53
10	2.33	3.04	1.97e-1	0.62	10.11	8.86e-1	0.78
15	2.46	1.94	2.63e-1	0.64	11.37	7.03e-1	0.67
20	2.37	3.19	2.63e-1	0.64	13.97	1.09e-1	0.82
24	2.41	2.51	2.65e-1	0.66	12.34	2.42e-1	0.75

Table 2. Fitting results of the impedance spectra of NF616 in deep salt at 673 K.

4 Conclusions

The electrochemical impedance spectra for the corrosion of the alloy NF616 beneath fused ZnCl₂-KCl film at 673 K in air show the typical characteristics of a diffusion-controlled reaction, i.e., a small semicircle at high frequency and a line at low frequency. An equivalent circuit of double-layer capacitance parallel with charge-transfer resistance in series with a Warburg resistance can be used to describe the diffusion-controlled reaction. However, the electrochemical impedance spectra of the alloy in deep molten ZnCl₂-KCl presented the characteristics of two capacitive loops during the duration of the experimental test. An equivalent circuit of double layer capacitance at the localized corrosion zone parallel to scale capacitance can be set up to describe this impedance response. The corrosion of the alloy in deep salt is controlled by the supply of oxygen at the cathodic reaction. The different electrochemical impedance spectra under two corrosion conditions may be related to the different supply of oxygen. Besides, the tangential diffusion and dispersion effects are very obvious in molten-salt corrosion.

Acknowledgments

The authors acknowledge financial support by the Natural Scientific Foundation of Jiangsu Province, China under Contract SBK200930394, and by the High Education Natural Scientific Foundation of Jiangsu Province, China under Contract 08KJB430003.

References

- [1] H.J. Grabke, E. Reese and M. Spiegel, *Corros. Sci.*, 37 (1995), 1023–1043.
- [2] A. Nishikata, Y. Ichihara and T. Tsuru, Corros. Sci., 37 (1995), 897–911.
- [3] A. Nishikata, Y. Ichihara and T. Tsuru, *Electrochim. Acta*, 41 (1996), 1057–1062.
- [4] H. Numata, N. Yamanouchi, K. Nunomura, M. Tamura, I. Matsushima and S. Haruyama, *Journal of Japan Institute of Metals*, 51 (1987), 342–349.
- [5] C. L. Zeng, W. Wang and W. T. Wu, Corros. Sci., 43 (2001), 787–801.
- [6] T. J.Pan, W. M.Lu, Y. J.Ren, W. T. Wu and C. L. Zeng, Oxid. Met., 72 (2009), 179–190.
- [7] G. Gao, F. H. Stott, J. L. Dawson and D. M. Farrel, Oxid. Met., 33 (1990), 79–94.
- [8] Y. M. Wu and R. A. Rapp, J. Electrochem. Soc., 138 (1991), 2683–2690.
- [9] C.L. Zeng and T. Zhang, *Electrochim. Acta.*, 49 (2004), 1429–1433.
- [10] C. L. Zeng and J. Li, Electrochim. Acta, 50 (2005), 5533– 5538.
- [11] T. J.Pan, Y. F. Lin, J.Hu and C. L. Zeng, *High Temp. Mater. Proc.*, 28 (2009), 233–244.
- [12] Y. S. Li, Y. Niu and W. T. Wu, Mater. Sci. Eng., A345 (2003), 64–71.
- [13] Y, Ihara, H. Ohgame, K. Sakiyama, and K. Hashimoto, Corros. Sci., 21 (1981), 805–817.
- [14] Z. A. Foroulis, ANTI-Corrosion, 1 (1988), 4–12.